Supplementary materials

Stocking density-driven shift of atmospheric carbon dioxide source-sink functions in mussel culture systems

Miao-Jun Pan[1], Yu-Xi Zhao[1], Sheng-Jie Xu[1], Chang-Lin Li[1,2], Zhou Zhang[1], Shuang-Jie Tian[1], Xiang-Li Tian[1], Yan-Gen Zhou[1], Yun-Wei Dong[1], Li Li[1*], Shuang-Lin Dong[1*]

[1]Key Laboratory of Mariculture of Ministry of Education, Fisheries College, Ocean University of China, Qingdao 266003, China;

[2]South China Sea Fisheries Research Institute, Chinese Academy of Fishery Sciences, Guangzhou 510300, PR China;

*Corresponding author: Shuang-Lin Dong and Li Li

E-Mail address: dongsl@ouc.edu.cn; l_li@ouc.edu.cn

Running Title: Stocking density-driven shift in CO_2 removal of mussel culture ecosystems

Contents

Supplementary Methods

Supplementary Method 1 | Calculation of CO_2 flux at the water-air interface

Then, CO_2 flux at the air-water interface ($FCO_{2\text{-aw}}$) was estimated using the thin boundary layer model:

$$FCO_{2\text{-aw}} = k \times K_0 \times (pCO_{2w} - pCO_{2A})$$

Where K_0 is the solubility coefficient of CO_2 in water, which depends on temperature and salinity[1]. pCO_{2w} and pCO_{2A} denote the pCO_2 in surface water and in the atmosphere. pCO_{2A} was determined from air samples collected above the mesocosms. k is the gas transfer velocity of CO_2 (cm h^{-1}), expressed as[2]:

$$k = 0.251 \times U^2 \times \left(\frac{Sc}{660}\right)^{-0.5}$$

where U (m s^{-1}) is the wind speed at 10 m above ground; Sc denotes the Schmidt number (dimensionless), which varies with temperature (T, °C) and can be calculated as follows [2]:

$$Sc = 2116.8 - 136.25T + 4.7353T^2 - 0.092307T^3 + 0.0007555T^4$$

Supplementary Method 2 | Determination of CO_2 concentration in overlying water and porewater and calculation of CO_2 flux at the sediment-water interface

Dissolved CO_2 concentrations in the overlying water were determined using the headspace gas chromatography method[3,4]. Specifically, 100 mL overlying water sample was collected using a 200-mL syringe equipped with a three-way valve and connected to a long silicone tube. Immediately, 100 mL of high-purity N_2 (> 99.99%) was injected into the syringe. Then, the mixture was vigorously shaken for 10 minutes and then allowed to stand for 20 minutes. The headspace gas was subsequently transferred into a pre-evacuated gas sampling bag and analyzed for CO_2 concentration using a gas chromatograph (8860GC, Agilent Technologies, USA) equipped with a thermal conductivity detector (TCD). Dissolved CO_2 concentrations were calculated according to Henry's law, accounting for water temperature, salinity and headspace ratio[1,5].

Porewater CO_2 concentrations were determined following a similar procedure[6,7]. Surface sediments were collected with a gravity corer, and the top 4 cm of each core was subdivided into 2-cm intervals. From each interval, 50 mL of sediment was collected using a syringe with a cut tip (2 cm in diameter) and transfer into a 250 mL glass bottle containing 100 mL of mesocosm surface water. The bottle was immediately sealed with a butyl rubber stopper. After shaking for 10 minutes and settling for 20 minutes, the headspace gas was displaced by injecting an equal volume of water and then collected in pre-evacuated gas sampling bags. The CO_2 concentration in the headspace was measured via gas chromatography with a TCD and converted to dissolved CO_2 concentration in porewater following established methods[8].

The CO_2 flux at the sediment-water interface ($F\mathrm{CO}_{2\text{-sw}}$) was estimated using Fick's first law, which models molecular diffusion based on the concentration gradient between porewater and overlying water[9,10]:

$$F\mathrm{CO}_{2\text{-sw}} = -\phi \times \frac{\mathrm{D_S}}{\theta^2} \times \frac{\mathrm{d_c}}{\mathrm{d_z}}$$

Where ϕ is the sediment porosity, determined from cutting-ring samples and calculated from the weight loss after drying at 105°C for 24 h[11]; θ^2 is the corrected curvature, calculated by the formula $\theta^2 = 1 - \ln(\phi)$[12]; D_S (m^2 s^{-1}) is the diffusion coefficient of CO_2 in water and varies with temperature[13]; d_c/d_z (mmol m^{-4}) is the vertical gradient of dissolved CO_2 concentration at the sediment-water interface.

Supplementary Method 3 | Calculation of mussel metabolic activity rates

The DO consumption rate (R_{DO}, μmol O_2 g^{-1} h^{-1}) and TAN excretion rate (R_{TAN}, μmol N g^{-1} h^{-1}) of mussels are calculated based on the following formula:

$$R_{DO} \text{ or } R_{TAN} = \frac{(C_f - C_i - \Delta C_0) \times V}{T \times M}$$

In the formula, C_i and C_f denote the initial and final DO or TAN concentrations (μmol O_2 L^{-1} or μmol N L^{-1}) in the incubation water, respectively; ΔC_0 denote the change in DO or TAN concentration in the control chambers over the incubation period; V is the volume of incubation water (L); T is the experimental duration (h), and M is the dry weight of mussel soft tissue (g).

Calcification rate (R_{cal}, μmol $CaCO_3$ g^{-1} h^{-1}) was determined using the alkalinity anomaly technique[14], with a correction for changes in TA due to ammonia excretion[15]. The rate was calculated as follows:

$$R_{cal} = \frac{[-(TA_f - TA_i - \Delta TA_0) + \Delta TAN] \times V}{2 \times T \times M}$$

In the formula, TA_i and TA_f represent the TA of the incubation water before and after incubation, respectively; ΔTA_0 indicates the change in TA observed in the control chambers; ΔTAN denotes the change in TAN concentration during the incubation. It is assumed that for every 1mol of ammonia nitrogen produced, the total alkalinity will decrease by 1mol.

The calculation formula for the respiration rates (R_{res}, μmol CO_2 g^{-1} h^{-1}) of mussels is as follows:

$$R_{res} = \frac{[(\Delta TA)/2 + (DIC_f - DIC_i - \Delta DIC_0)] \times V}{T \times M}$$

In the formula, ΔTA represents the change in TA during the incubation; DIC_i and DIC_f represent the DIC concentrations in the water before and after incubation, respectively; ΔDIC_0 indicates the change in DIC observed in the control chambers.

Supplementary Method 4 | Quantify the contributions of different biogeochemical processes to changes in carbonate parameters

Following the method proposed by previous studies[16-18], a mass balance model was employed to quantify the contributions of different biogeochemical processes to net changes in carbonate parameters (TA, DIC and pCO_2) at 10-day intervals, in order to identify the key processes that control CO_2 source-sink function of bivalve culture systems. Suppose that the initial values of water temperature, salinity and carbonate parameters are defined as T_1, S_1, TA_1, DIC_1 and $(pCO_2)_1$, respectively. After 10 days, these values become T_2, S_2, TA_2, DIC_2 and $(pCO_2)_2$.

The primary processes controlling changes in TA

In this study, the effects of net primary production (NPP) and bivalve calcification on TA are taken into account.

$$\Delta TA = TA_2 - TA_1 = \Delta TA_{NPP} + \Delta TA_{cal} + \Delta TA_{others}$$

In the formulation, ΔTA_{NPP} denotes the contribution of the water column NPP to net changes in TA, and it is estimated based on the relationship between the net oxygen production and the net change in TA during photosynthesis[19]. ΔTA_{cal} denotes the contribution of calcification to net changes in TA, estimated from the calcification rate measured in the mussel incubation experiment. ΔTA_{others} denotes the contribution of other processes to net changes in TA, calculated as ΔTA minus ΔTA_{NPP} and ΔTA_{cal}.

The primary processes controlling changes in DIC

In this study, the effects of CO_2 fluxes at the air-water interface ($FCO_{2\text{-aw}}$), CO_2 fluxes at the sediment-water interface ($FCO_{2\text{-sw}}$), NPP, calcification and respiration on DIC were considered.

$$\Delta DIC = DIC_2 - DIC_1 = \Delta DIC_{FCO2\text{-aw}} + \Delta DIC_{FCO2\text{-sw}} + \Delta DIC_{NPP} + \Delta DIC_{res} + \Delta DIC_{cal} + \Delta DIC_{others}$$

In the formulation, $\Delta DIC_{FCO2\text{-aw}}$ and $\Delta DIC_{FCO2\text{-sw}}$ represent the contributions of $FCO_{2\text{-aw}}$ and $FCO_{2\text{-sw}}$ to the net change in DIC, respectively. ΔDIC_{NPP} represents the contribution of the water column NPP to the net change in DIC, estimated from the relationship between the net oxygen production and net CO_2 consumption during photosynthesis[19]. ΔDIC_{res} and ΔDIC_{cal} represent the contributions of bivalve respiration and calcification to the net change in DIC, estimated from the respiration rates and calcification rates measured in the mussel incubation experiment, respectively. ΔDIC_{others} represents the contribution of other processes to the net change in DIC, the residual after subtracting the contributions of the known processes from ΔDIC.

The primary processes controlling changes in pCO_2

In this study, the effects of temperature, salinity, $FCO_{2\text{-aw}}$, $FCO_{2\text{-sw}}$, NPP, respiration and calcification on pCO_2 were considered.

$$\Delta pCO_2 = (pCO_2)_2 - (pCO_2)_1 = \Delta(pCO_2)_{tem} + \Delta(pCO_2)_{sal} + \Delta(pCO_2)_{FCO2\text{-aw}} + \Delta(pCO_2)_{FCO2\text{-sw}} + \Delta(pCO_2)_{NPP} + \Delta(pCO_2)_{res} + \Delta(pCO_2)_{cal} + \Delta(pCO_2)_{others}$$

$$\Delta(pCO_2)_{tem} = f\,(T_2, S_1, TA_1, DIC_1) - (pCO_2)_1$$

$$\Delta(pCO_2)_{sal} = f\,(T_1, S_2, TA_1, DIC_1) - (pCO_2)_1$$

$$\Delta(pCO_2)_{FCO2\text{-}aw} = f\left(T_1, S_1, TA_1, (DIC_2)_{FCO2\text{-}aw}\right) - (pCO_2)_1$$

$$\Delta(pCO_2)_{FCO2\text{-}sw} = f\left(T_1, S_1, TA_1, (DIC_2)_{FCO2\text{-}sw}\right) - (pCO_2)_1$$

$$\Delta(pCO_2)_{NPP} = f\left(T_1, S_1, (TA_2)_{NPP}, (DIC_2)_{NPP}\right) - (pCO_2)_1$$

$$\Delta(pCO_2)_{res} = f\left(T_1, S_1, (TA_2)_{res}, (DIC_2)_{res}\right) - (pCO_2)_1$$

$$\Delta(pCO_2)_{cal} = f\left(T_1, S_1, (TA_2)_{cal}, (DIC_2)_{cal}\right) - (pCO_2)_1$$

In the formulation, $(\triangle pCO_2)_{tem}$, $(\triangle pCO_2)_{sal}$, $(\triangle pCO_2)_{FCO2\text{-}aw}$, $(\triangle pCO_2)_{FCO2\text{-}sw}$, $(\triangle pCO_2)_{NPP}$, $(\triangle pCO_2)_{res}$, $(\triangle pCO_2)_{cal}$ and $(\triangle pCO_2)_{others}$ denote the contributions of temperature, salinity, $FCO_{2\text{-}aw}$, $FCO_{2\text{-}sw}$, NPP, calcification, respiration and other processes to the net change in pCO_2, respectively. $(DIC_2)_{FCO2\text{-}aw}$, $(DIC_2)_{FCO2\text{-}sw}$, $(TA_2)_{NPP}$, $(DIC_2)_{NPP}$, $(TA_2)_{res}$, $(DIC_2)_{res}$, $(TA_2)_{cal}$, $(DIC_2)_{cal}$ denote the TA or DIC values at T2 when the corresponding process works alone. f () denotes the pCO_2 under the given environmental and carbonate parameters, calculated using the CO2SYS program[20].

Supplementary Figures

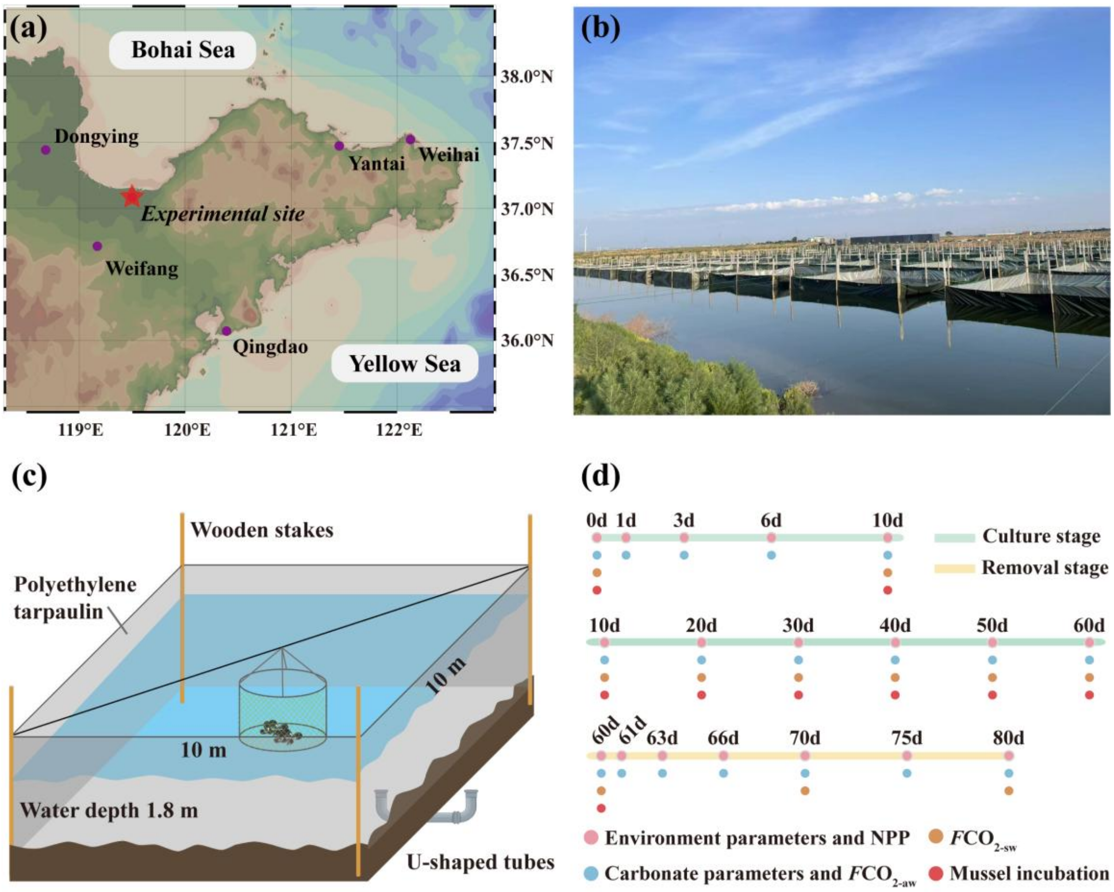

Supplementary Figure 1 | Experimental mesocosms and sampling campaign. (a) Location of the experimental site. (b) Field photograph of the mesocosms. (c) Schematic diagram of the mesocosms. (d) Sampling schedule and measured indicators.

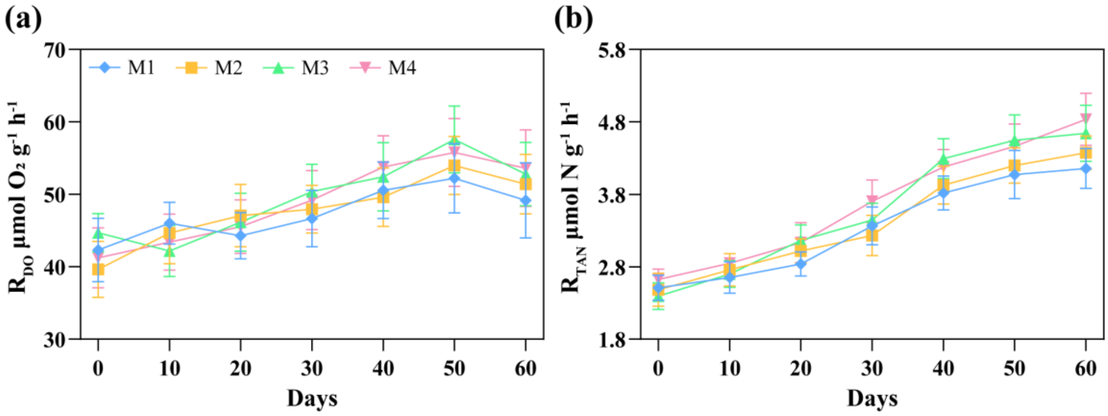

Supplementary Figure 2 | The metabolic activity rates of mussels. (a) The dissolved oxygen consumption rate (R_{DO}) of mussels at different culture period. (b) The total ammonia nitrogen (R_{TAN}) excretion rate of mussels at different culture period. The error bars represent the standard deviation.

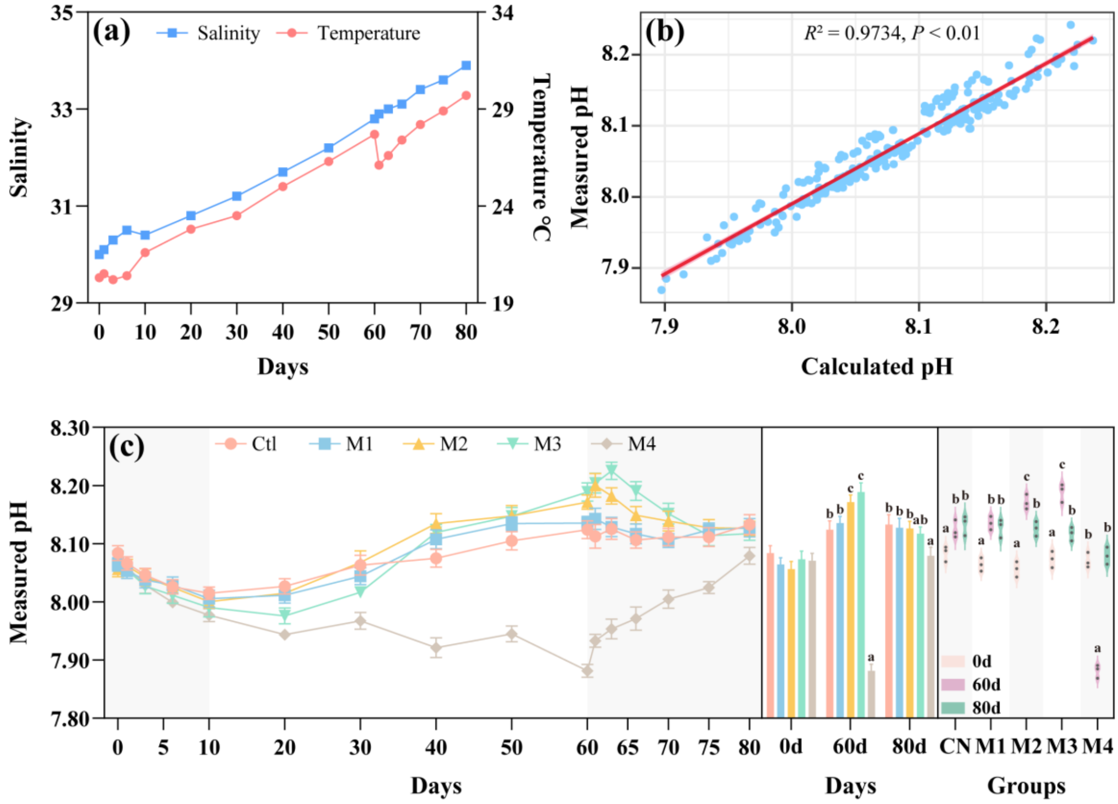

Supplementary Figure 3 | Environmental parameters of mussel culture systems during the experiment. (a) Variations in salinity and temperature of the surface water. (b) Correlation between measured pH and calculated pH. (c) Variations in pH of the surface water. The error bars represent the standard deviation. Different letters indicate significant differences between data from different groups ($P < 0.05$).

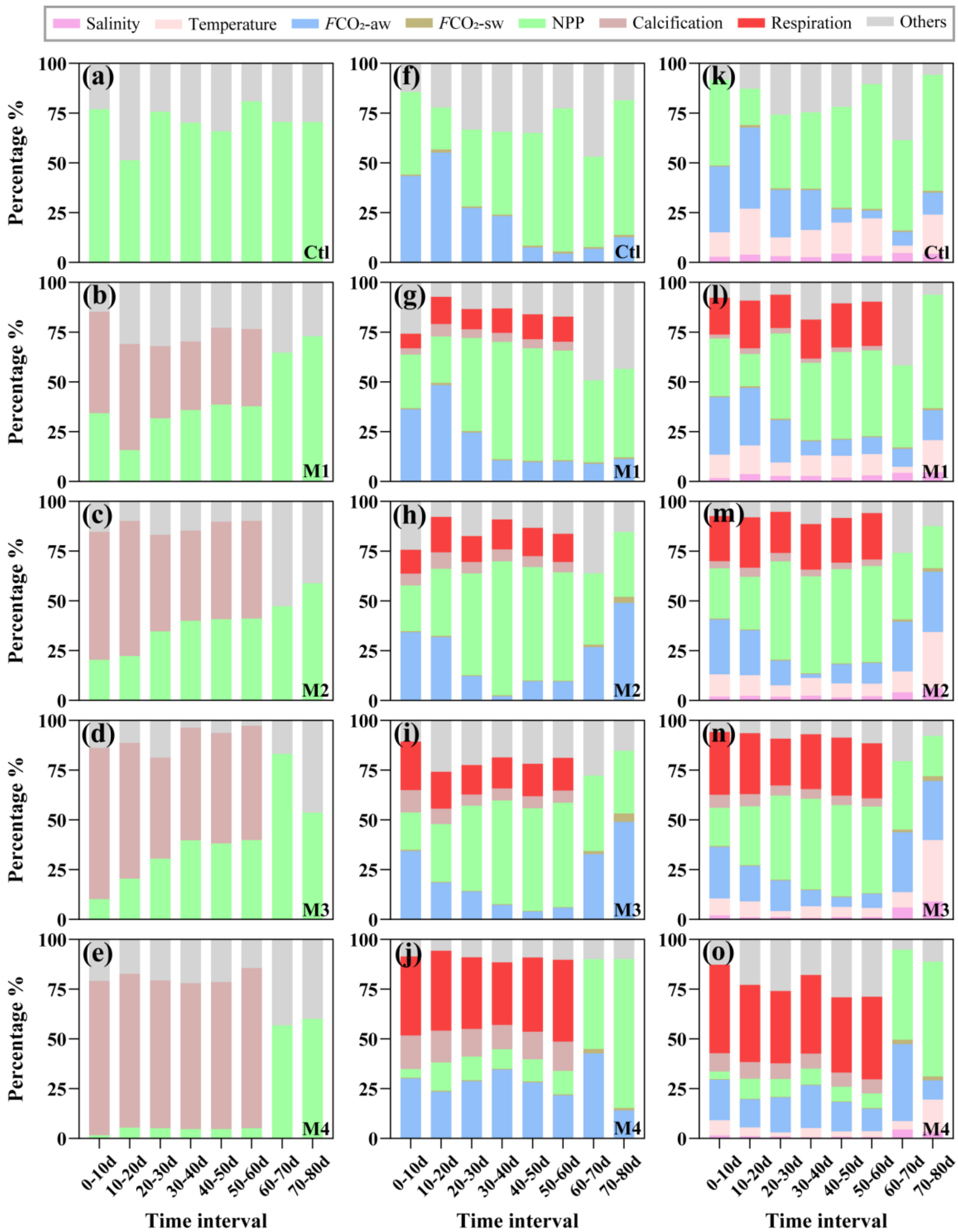

Supplementary Figure 4 | Proportion of different ecological processes in the total absolute contributions to changes in carbonate parameters. (a-e) Proportion of different ecological processes in the total absolute contributions to TA change. (f-j) Proportion of different ecological processes in the total absolute contributions to DIC change. (k-o) Proportion of different ecological processes in the total absolute contributions to *p*CO_2 change.

Supplementary Tables

Supplementary Table 1 | Stocking densities in coastal bivalve culture farms worldwide

Systems	Country	Area km^2	Water volume m^3	Exchange water volume m^3	Main bivalve species	Stock capacity g (survey year)	Stock density g m^{-3}	Adjusted stock density g m^{-3}	References
Mesocosms	-	100 m^2	180	-	mussel	-	-	6.94 ~ 55.56	This study
Zhangzidao sea area	China	333	1.17×10^{10}	5.03×10^{11}	scallop	124725 (2010)	10.70	0.25	21-23
Oosterschelde estuary	Netherlands	350	2.48 ~ 3.15×10^{9}	1.20 ~ 1.44×10^{10}	oyster, mussel, calm	134030 (2009)	42.55 ~ 54.04	9.30 ~ 11.19	24,25
Sacca di Goro lagoon	Italy	26	3.90×10^{7}	4.75×10^{9}	calm	11250 (2001)	288.46	2.37	26,27
Ria de Aveiro lagoon	Portugal	74.5	7.45×10^{7}	9.85×10^{8} ~ 2.80×10^{9}	calm	28404 (2012)	381.26	10.13 ~ 28.83	28-30
Thau lagoon	France	68	2.72×10^{8}	2.03×10^{9}	oyster, mussel	25433 (2016)	93.50	12.50	31
Sishili Bay	China	133	1.20×10^{9}	5.75×10^{10}	scallop	30000 (2009)	25.06	0.52	32
Sechura Bay	Peru	400	2.00×10^{8}	2.76 ~ 4.14×10^{11}	scallop	58955 (2010)	9.83	014 ~ 0.21	33
Dapeng Cove	China	14	9.80×10^{7}	1.49×10^{9}	oyster	12100 (2012)	61.73	4.06	34-36
Malpeque Bay	Canada	223..6	6.30×10^{8}	6.38×10^{10}	mussel, oyster	5689 ~ 10169 (2014)	9.04~16.15	0.09 ~ 0.16	37,38
Sanggou Bay	China	144	1.08×10^{9}	3.27×10^{10}	oyster, scallop	97848 (2016)	90.60	2.99	39-41

Note: The water volume of each culture system was obtained from the literature or calculated from area and mean water depth. The Exchange water volume was calculated from the water volume and the annual number of turnovers. Stocking capacity were taken from the literature or calculated from annual production (tons per year) and the culture cycle (year). Stocking density was calculated as the stocking capacity divided by the water volume, and the adjusted stocking density as the stocking capacity divided by the exchange water volume.

Reference

1 Weiss, R. F. Carbon dioxide in water and seawater: the solubility of a non-ideal gas. *Mar. Chem.* **2**, 203–215 (1974).

2 Wanninkhof, R. Relationship between wind speed and gas exchange over the ocean revisited. *Limnol. Oceanogr. Meth.* **12**, 351–362 (2014).

3 Zhang, W. S., Li, H. P., Xiao, Q. T. & Li, X. Y. Urban rivers are hotspots of riverine greenhouse gas (N_2O, CH_4, CO_2) emissions in the mixed-landscape chaohu lake basin. *Water Res.* **189**, 116624 (2021).

4 Yuan, D. N. *et al.* Nitrogen addition effect overrides warming effect on dissolved CO_2 and phytoplankton structure in shallow lakes. *Water Res.* **244**, 120437 (2023).

5 Tang, W., Xu, Y. J., Ni, M. F. & Li, S. Y. Land use and hydrological factors control concentrations and diffusive fluxes of riverine dissolved carbon dioxide and methane in low-order streams. *Water Res.* **231**, 119615 (2023).

6 Donis, D. *et al.* Full-scale evaluation of methane production under oxic conditions in a mesotrophic lake. *Nat. Commun.* **8**, 1661 (2017).

7 Tang, L. L. *et al.* Seasonal variations in source-sink balance of CO_2 in subtropical earthen aquaculture ponds: Implications for carbon emission management. *J. Hydrol.* **626**, 130330 (2023).

8 Yang, P., Lai, D. Y. F., Yang, H. & Tong, C. Carbon dioxide dynamics from sediment, sediment-water interface and overlying water in the aquaculture shrimp ponds in subtropical estuaries, southeast China. *J. Environ. Manage.* **236**, 224–235 (2019).

9 D'Ambrosio, S. L. & Harrison, J. A. Measuring CH_4 fluxes from lake and reservoir sediments: Methodologies and needs. *Front. Environ. Sci.* **10**, 850070 (2022).

10 Sun, H. Y. *et al.* Drivers of spatial and seasonal variations of CO_2 and CH_4 fluxes at the sediment water interface in a shallow eutrophic lake. *Water Res.* **222**, 118916 (2022).

11 Zhang, L. *et al.* Pore water nutrient characteristics and the fluxes across the sediment in the Pearl River estuary and adjacent waters, China. *Estuar. Coast. Shelf Sci.* **133**, 182–192 (2013).

12 Boudreau, B. P. *Diagenetic models and their implementation*. (Springer Berlin, 1997).

13 Broecker, W. S. & Peng, T.-H. Gas exchange rates between air and sea. *Tellus* **26**, 21–35 (1974).

14 Smith, S. & Key, G. Carbon dioxide and metabolism in marine environments. *Limnol. Oceanogr.*, 493–495 (1975).

15 Gazeau, F., Urbini, L., Cox, T. E., Alliouane, S. & Gattuso, J. P. Comparison of the alkalinity and calcium anomaly techniques to estimate rates of net calcification. *Mar. Ecol.-Prog. Ser.* **527**, 1–12 (2015).

16 Xue, L. *et al.* Sea surface carbon dioxide at the Georgia time series site (2006-2007): Air-sea flux and controlling processes. *Prog. Oceanogr.* **140**, 14–26 (2016).

17 Xue, L., Cai, W. J., Sutton, A. J. & Sabine, C. Sea surface aragonite saturation state variations and control mechanisms at the Gray's Reef time-series site off Georgia, USA (2006–2007). *Mar. Chem.* **195**, 27–40 (2017).

18 Yang, B. *et al.* Massive shellfish farming might accelerate coastal acidification: A case study on carbonate system dynamics in a bay scallop (*Argopecten irradians*) farming area, North Yellow Sea. *Sci. Total Environ.* **798**, 149214 (2021).

19 Yin, H., Jin, L. & Hu, X. P. Interpreting biogeochemical processes through the relationship between total alkalinity and dissolved inorganic carbon: Theoretical basis and limitations. *Limnol. Oceanogr. Meth.* **22**, 311–320 (2024).

20 Pierrot, D., Wallace, D. & Lewis, E. *MS Excel program developed for* CO_2 *system calculations*. (Carbon dioxide information analysis center, 2006).

21 Dong, S. L., Tian, X. L., Gao, Q. F. & Dong, Y. W. *Aquaculture Ecology*. (Springer Nature Singapore, 2023).

22 Yu, Y., Zhang, W., Wang, S. & Xiao, T. Abundance and biomass of planktonic ciliates in the sea area around Zhangzi Island, Northern Yellow Sea. *Acta Ecologica Sinica* **33**, 45–51 (2013).

23 Zhang, J. H., Fang, J. G. & Wang, S. H. Carrying capacity for Patinopecten yessoensis in Zhang Zidao Island, China. *Journal of Fisheries of China* **32**, 236–241 (2008).

24 Jiang, L., Soetaert, K. & Gerkema, T. Decomposing the intra-annual variability of flushing characteristics in a tidal bay along the North Sea. *J. Sea Res.* **155**, 101821 (2019).

25 Jiang, L., Gerkema, T., Wijsman, J. W. M. & Soetaert, K. Comparing physical and biological impacts on seston renewal in a tidal bay with extensive shellfish culture. *J. Mar. Syst.* **194**, 102–110 (2019).

26 Zaldívar, J. M. *et al.* Long-term simulation of main biogeochemical events in a coastal lagoon: Sacca Di Goro (Northern Adriatic Coast, Italy). *Cont. Shelf Res.* **23**, 1847–1875 (2003).

27 Turolla, E., Castaldelli, G., Fano, E. A. & Tamburini, E. Life cycle assessment (LCA) proves that Manila clam farming (*Ruditapes Philippinarum*) is a fully sustainable aquaculture practice and a carbon sink. *Sustainability-Basel* **12**, 5252 (2020).

28 Jiang, W. W. *et al.* A food-web model as a tool for the ecosystem-level management of bivalves in an Atlantic coastal lagoon. *Mar. Environ. Res.* **190**, 106117 (2023).

29 Velez, C., Figueira, E., Soares, A. & Freitas, R. Spatial distribution and bioaccumulation patterns in three clam populations from a low contaminated ecosystem. *Estuar. Coast. Shelf Sci.* **155**, 114–125 (2015).

30 Vaz, L., Sousa, M. C., Gómez-Gesteira, M. & Dias, J. M. Water renewal estimation for sustainable aquaculture development in Ria de Aveiro and Rias Baixas. *Reg. Stud. Mar. Sci.* **49**, 102098 (2022).

31 Pete, R. *et al.* A box-model of carrying capacity of the Thau lagoon in the context of ecological status regulations and sustainable shellfish cultures. *Ecol. Model.* **426**, 109049 (2020).

32 Wang, Y. J., Liu, D. Y., Dong, Z. J., Di, B. P. & Shen, X. H. Temporal and spatial distributions of nutrients under the influence of human activities in Sishili Bay, northern Yellow Sea of China. *Mar. Pollut. Bull.* **64**, 2708–2719 (2012).

33 Kluger, L. C., Taylor, M. H., Mendo, J., Tam, J. & Wolff, M. Carrying capacity simulations as a tool for ecosystem-based management of a scallop aquaculture system. *Ecol. Model.* **331**, 44–55 (2016).

34 Wang, C., Lin, J., Chen, P. M. & Zhang, S. Y. Numerical simulation of annual average wind's impact on water exchange in Daya Bay. *Journal of Shanghai Ocean University* **18**, 351–358 (2009).

35 Yu, Z. H., Jiang, T., Xia, J. J., Ma, Y. E. & Zhang, T. Ecosystem service value assessment for an oyster farm in Dapeng Cove. *Journal of Fisheries of China* **38**, 853–860 (2014).

36 Xu, Y., Li, S. L., Chen, J. L. & Cui, Z. G. Assessment of mariculture-derived microplastic pollution in Dapeng Cove, China. *Front. Mar. Sci.* **11**, 1382249 (2024).

37 Bacher, C., Filgueira, R. & Guyondet, T. Probabilistic approach of water residence time and connectivity using Markov chains with application to tidal embayments. *J. Mar. Syst.* **153**, 25–41 (2016).

38 Lavaud, R., Guyondet, T., Filgueira, R., Tremblay, R. & Comeau, L. A. Modelling bivalve culture - Eutrophication interactions in shallow coastal ecosystems. *Mar. Pollut. Bull.* **157**, 111282 (2020).

39 Zhang, J. H. *et al.* Sediment-focused environmental impact of long-term large- scale marine bivalve and seaweed farming in Sungo Bay, China. *Aquaculture* **528**, 735561 (2020).

40 He, Y. Q., Xuan, J. L., Ding, R. B., Shen, H. & Zhou, F. Influence of Suspended Aquaculture on Hydrodynamics and Nutrient Supply in the Coastal Yellow Sea. *J. Geophys. Res.-Biogeosci.* **127** (2022).

41 Gao, Y. P. *et al.* Simulation of oyster ecological carrying capacity in Sanggou Bay in the ecosystem context. *Aquac. Int.* **28**, 2059–2079 (2020).